

CTuF7 Fig. 1. Contributions to acousto-photonic signal for three different receiver locations.

original photon density wave is incident from the left. In the first frame, the receiver is located at (0, 2.5 cm, 0), which is directly opposite the ultrasound focus. The integrand is symmetric in z , and is strongest at the origin, as expected. When the receiver is moved to (0, 2.5 cm, 1.25 cm) and then to (0, 2.5 cm, 2.5 cm), the peak shifts slightly toward the receiver, and a secondary peak develops near $z = 2.5$ cm. The secondary peak has an amplitude about 20% of the first. The size of the primary peak is a few wavelengths in all cases.

To a good approximation, the acousto-photonic imager behaves as expected, in that the signal arises predominantly at the waist of the ultrasound beam. The dimensions of the peak are of the order of the ultrasound wavelength, as expected. However, the PSF is pulled and broadened as the receiver moves away from a position near the ultrasound focus. A broad secondary peak develops in the ultrasound beam between the source and receiver. The possibility then exists for confusing strongly scattering objects at the secondary peak with weakly scattering objects at the primary one. Inversion algorithms must be able to address this issue, and multiple receivers may help in optimizing the resolution of acousto-photonic imagers.

1. D.A. Boas, L.E. Campbell, A.G. Yodh, *Phys. Rev. Lett.* **75**, 1855–1858 (1995).
2. Lihong Wang, Steven L. Jacques, Xuemei Zhao, *Opt. Lett.* **20**, 629–631 (1995).
3. O.P. Svaasand, and B.K. Tromberg, in *Future Trends of Biomedical Applications of Lasers*, Proc. SPIE 1525, 41–50 (1991).

CTuG 10:30 am–12:00 pm
Room 100

Tunable Diode Laser Sensors

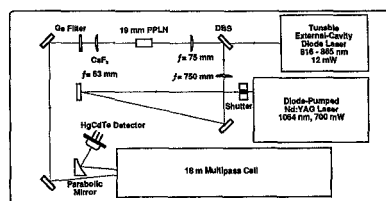
James B. Abshire, NASA Goddard Space Flight Center, *Presider*

CTuG1 (Invited) 10:30 am

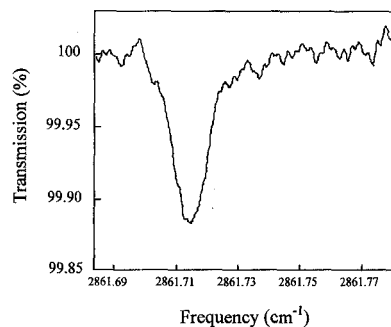
Tunable mid-infrared laser-based gas sensors: new technologies and applications

David G. Lancaster, Frank K. Tittel, Dirk Richter, K.P. Petrov,* Robert F. Curl, *Rice Quantum Institute, Rice University, Houston, Texas 77251-1892; E-mail: fkt@rice.edu*

This work describes the design and performance characteristics of room-temperature



CTuG1 Fig. 1. Scaled diagram of the compact (30 cm × 61 cm) diode-pumped difference-frequency spectrometer for multicomponent trace gas detection.



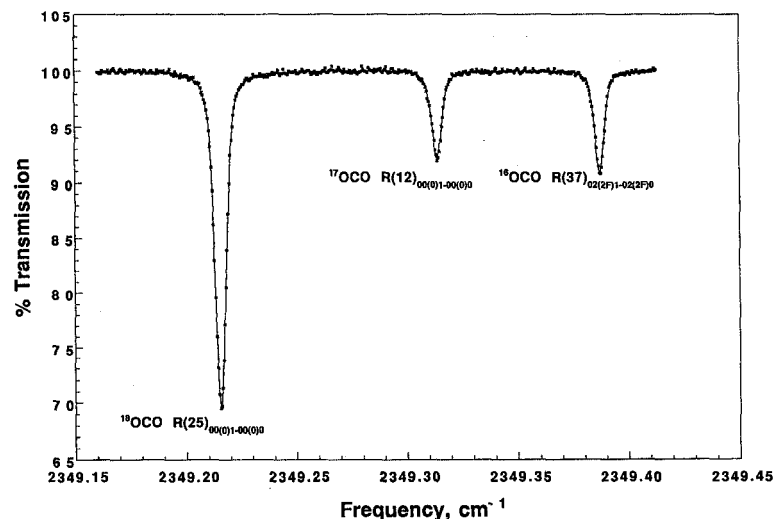
CTuG1 Fig. 2. A trace of 230 ppb formaldehyde in ambient air. A minimum detectable concentration of 30 ppb was determined.

mid-infrared diode-pumped sensors capable of either single or multicomponent real-time trace gas detection in ambient air. The difference-frequency-generation-(DFG) based sensor technology employs periodically poled lithium niobate (PPLN) crystals with multiple grating periods pumped by two single-frequency solid-state lasers and a thermoelectrically cooled HgCdTe infrared detector.^{1–3} For single or dual component target gas concentration measurements, the spectroscopic DFG source is pumped by two compact lasers, a 50 to 100 mW single-frequency GaAlAs diode laser in the 800 to 865 nm region and a single-frequency monolithic ring Nd:YAG laser at 1064 nm. For

multicomponent trace gas detection, the solitary diode laser was replaced by a 16-mW tunable external-cavity diode laser (Fig. 1). Tuning of the output wavelength from 840 nm to 865 nm was accomplished by rotation of its external diffraction grating. Continuous linear frequency scans of up to 80 GHz were performed by fine adjustment of the grating angle with a piezo-electric actuator, driven by a 50-Hz triangular wave.

Two different configurations were used for the optical path through the gas sample. In the open path configuration, a collimated DFG beam was returned to the source by a hollow corner cube retro-reflector with a circular aperture of 6.3 cm. The corner cube was placed at a distance of 2 to 9 m from the receiving mirror. Adjustment of the mirror tilt was used to point the DFG beam at the center of the corner cube for optimization of optical throughput, typically 80%. This arrangement allowed path-integrated measurements of trace gas concentration in open air at atmospheric pressure. Another sampling configuration employed a compact multipass absorption cell with an effective path length of 18 m. The cell could be connected to a pump and used for trace gas measurements in air at reduced pressure if necessary. Both sampling configurations provided a small free space after the turning mirror, sufficient to house a 10-cm-long reference absorption cell. Such an arrangement allowed the acquisition of absorption spectra of a sample gas overlapped with a Doppler-limited spectrum of a reference gas for wavelength calibration.

The broad continuous tuning range available with some commercial ECDLs, when used in the difference-frequency setup, makes it possible to cover idler wavelengths from 3.5 μm to 4.7 μm . This wavelength range contains strong fundamental rovibrational absorption bands of several important trace air contaminants, including carbon monoxide (CO), nitrous oxide (N_2O), carbon dioxide (CO_2), formaldehyde (H_2CO), monomethylhydrazine ($\text{N}_2\text{H}_3\text{CH}_3$), and methane (CH_4).



CTuG1 Fig. 3. Mid-infrared spectrum of the oxygen isotopes of CO_2 in room air at 3.6 kPa inside an 18 m multipass cell. The spectrum was acquired in 2 seconds and is a 100 sweep average.

Detection and measurement of these and other species in air are therefore possible with the use of a single DFG-based gas sensor.

Shown in Fig. 2 is a typical absorption spectrum of 230 ppb formaldehyde in air at 50% relative humidity. Residual low frequency interference fringes in the baseline are apparent with a peak-to-peak magnitude equivalent to ~ 30 ppb of H_2CO in ambient air. Increased sensitivity at the ppb level should be attainable using software signal filtering and enhanced data acquisition techniques. We also demonstrated the simultaneous spectroscopic measurement of the $^{18}O/^{17}O/^{16}O$ isotopic ratios in atmospheric CO_2 . Figure 3 shows a transmission spectrum of room air at 3.6 kPa in the 18 m multipass cell.

A promising development of this technology would involve the use of quasi-phase-matched PPLN waveguides in conjunction with fiber-coupled low-power diode lasers. Arbore *et al.*,⁴ reported DFG conversion efficiencies of up to $8\% \cdot W^{-1}$ for adiabatically tapered periodically segmented PPLN waveguides. With such high conversion efficiency per device, one can obtain DFG output power approaching the 0.1 mW level with only 50 mW of pump and signal power. The use of fiber-coupled pump and signal lasers would allow construction of compact, rugged, alignment-free optical gas sensors.

The work was supported in part by the NASA Johnson Space Center, the Texas Advanced Technology Program, and the Robert A. Welch Foundation.

*Now with Gemfire, Palo Alto, California 94303

1. Th. Töpfer, K.P. Petrov, Y. Mine, D. Jundt, R.F. Curl, F.K. Tittel, *Appl. Opt.* **36**, 8042 (1997).
2. Y. Mine, N. Melander, D. Richter, D.G. Lancaster, K.P. Petrov, R.F. Curl, F.K. Tittel, to appear in *Appl. Phys. B* (December 1997).
3. K.P. Petrov, R.F. Curl, F.K. Tittel, accepted by *Appl. Phys. B* (October 1997).
4. M.A. Arbore, M.H. Chou, M.M. Fejer, in *Conference on Lasers and Electro-Optics*, Vol. 9 of 1996 OSA Technical Digest Series (Optical Society of America, Washington, D.C., 1996), p. 120.

CTuG2

11:00 am

Mid-infrared laser source for gas sensing based on waveguide difference-frequency generation

Douglas J. Bamford, Konstantin P. Petrov, Andrew T. Ryan, Thomas L. Patterson, Lee Huang, David Hui, Simon J. Field, Gemfire Corp., 2440 Embarcadero Way, Palo Alto, California 94303; E-mail: DJBAMFORD@AOL.COM

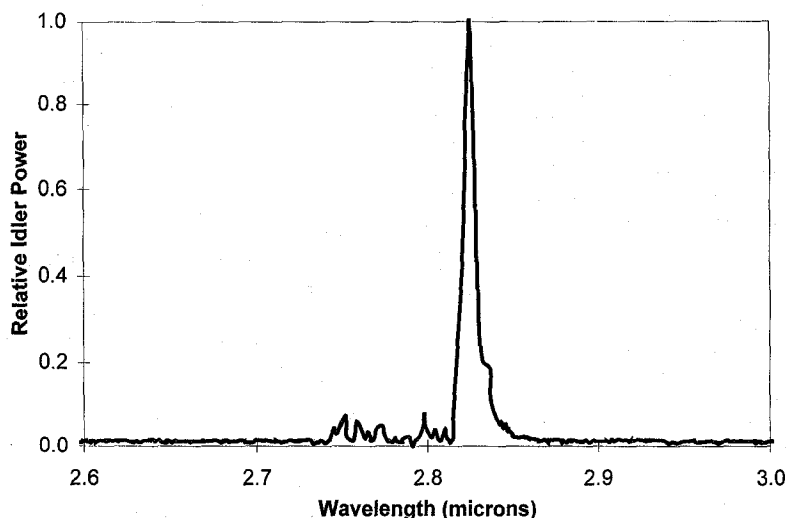
Compact, room-temperature mid-infrared laser sources have a variety of applications in gas detection. For example, many gases of importance for atmospheric science can be detected quantitatively using strong absorption lines in this spectral region. We have developed a room-temperature mid-IR laser source based on the frequency mixing of two diode lasers in

periodically poled lithium niobate (PPLN) waveguides. Output powers greater than $1 \mu W$ have been obtained. This laser source has been used to measure strong absorption lines of water vapor at $2.7 \mu m$. To our knowledge this is the first use of radiation generated in periodically poled waveguide structures for gas detection.

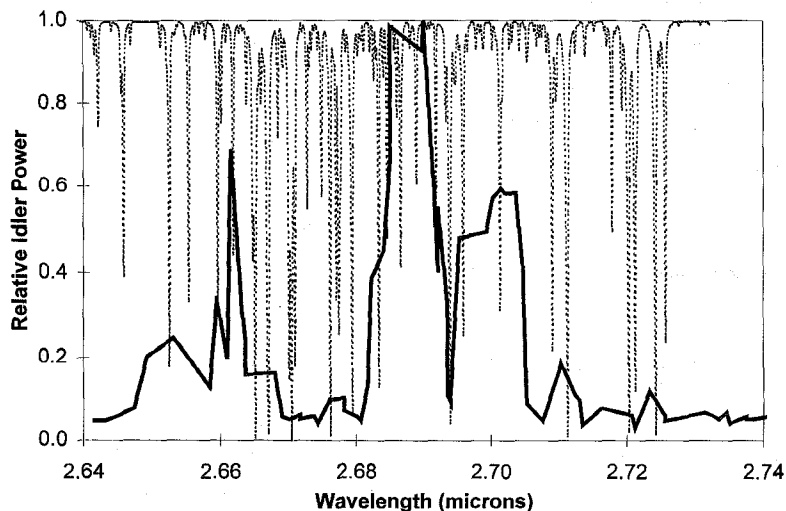
PPLN wafers with a variety of quasi-phase-matching (QPM) periods between $11.0 \mu m$ and $20.1 \mu m$ were fabricated using a patented electric field poling process.¹ Channel waveguides of various widths were then fabricated by annealed proton exchange; typical conditions included a 24-h exchange at $170^\circ C$ followed by a 30-h anneal at $340^\circ C$. The apparatus used for difference-frequency generation has been described previously.² Tunable radiation at $\lambda_1 = 715 \text{ nm}$ – 840 nm was provided by a Ti:sapphire laser pumped by an argon-ion laser. Fixed-frequency radiation at $\lambda_2 = 1010 \text{ nm}$ was provided by a grating-stabilized diode laser

(SDL-8630). The two laser beams were combined on a dichroic mirror and focused by a microscope objective into one of the PPLN waveguides. Powers of 30–50 mW from each laser could be coupled into a typical waveguide. The generated mid-IR radiation at λ_1 was collimated with a CaF_2 lens, passed through an interference filter with high transmission in the mid-infrared, and focused with a parabolic mirror onto a cryogenically cooled indium antimonide detector. The wavelength of the Ti:sapphire laser was changed using two different strategies: rotating an intracavity birefringent filter (for coarse tuning) and changing the tilt angle of an intracavity etalon (for fine tuning).

Figure 1 shows the generated power as a function of λ_1 in a $6\text{-}\mu m$ -wide waveguide with a QPM period of $15.5 \mu m$. The phase-matching curve deviates from the ideal sinc-squared shape because of the excitation of multiple waveguide modes. At the peak of the phase-matching curve ($\lambda_1 = 2.83 \mu m$) the



CTuG2 Fig. 1. Relative power as a function of idler wavelength in a $6\text{-}\mu m$ -wide waveguide with a QPM period of $15.5 \mu m$.



CTuG2 Fig. 2. Relative power as a function of idler wavelength in a $6\text{-}\mu m$ -wide waveguide with a QPM period of $15.0 \mu m$ (heavy solid line) along with a calculated absorption spectrum for atmospheric water vapor (dashed line).